https://doi.org/10.5194/egusphere-2025-4004
Preprint. Discussion started: 29 September 2025

Moisture storage, transport and mixing processes after sprinkler irrigation of Pasture cropland: Understanding based on water isotopes

Jiangwei Yang[a,b,c], *Guofeng Zhu*[a,b,c*], *Rui Li*[a,b,c], *Yinying Jiao*[a,b,c], *Xiaoyu Qi*[a,b,c], *Zhijie Zheng*[a,b,c], *Wenmin Li*[a,b,c], *Yani Gun*[a,b,c]

[a] *College of Geography and Environmental Science, Northwest Normal University, Lanzhou 730070, Gansu, China*

[b] *Shiyang River Ecological Environment Observation Station, Northwest Normal University, Lanzhou 730070, Gansu, China*

[c] *Key Laboratory of Oasis Resources and Environment and Sustainable Development in Gansu Province.*

[*] *Correspondence to: Guofeng Zhu (zhugf@nwnu.edu.cn)*

Abstract

The processes of water storage, migration, and mixing in agricultural fields are influenced by a combination of factors, including climatic conditions, soil properties, cropping structure, and field management practices. Sprinkler irrigation is a widely adopted method in agricultural fields globally. Studying the post-irrigation processes of sprinkler irrigation in specific regions can provide valuable insights for regional agricultural development and the conservation and utilization of water resources. In this study, we investigated the water storage, migration, and mixing processes in vegetation within arid irrigated areas. This was achieved by analyzing stable isotope data, using sprinkler-irrigated pastureland (alfalfa) as the research subject.The study

https://doi.org/10.5194/egusphere-2025-4004
Preprint. Discussion started: 29 September 2025

results indicated that: (1) there was significant isotope depletion in soil moisture following irrigation, with soil moisture and isotope characteristics returning to their pre-irrigation state after an average of 9 days; (2) water transport in the soil was predominantly vertical, with a minimal proportion of horizontal movement; and (3) evaporation losses due to sprinkler irrigation accounted for 32%, while losses from excess irrigation (infiltration into soil layers below 60 cm) comprised 5%. In arid regions, sprinkler irrigation effectively controls infiltration losses; however, evaporation losses remain considerably high. We recommend promoting low-level multipoint sprinkler irrigation and nighttime irrigation practices to enhance water use efficiency and ensure agricultural sustainability.

Key Words: Dry zone; stable isotopes; sprinkler-irrigated pasture; water transport

1.Introduction

Climate change and vegetation dynamics significantly impact the regional water cycle in arid irrigated areas (Zaitchik et al., 2023; Wang et al., 2024). Soil water, a vital component of the water cycle, can be replenished by precipitation or groundwater. Its storage, transport, and mixing processes are crucial for understanding the water cycle and water balance in arid regions (Chen et al., 2024). Stable isotope techniques, a powerful tool for tracing eco-hydrological features, have been widely utilized to study various processes, including evapotranspiration (Zhu et al., 2021), groundwater recharge (Koeniger et al., 2016), infiltration pathways (Dubbert et al., 2016; Zhu et al., 2021), evapotranspiration distribution (Gibson et al., 2021; Xiao et al., 2018), and plant water uptake (Rothfuss and Javaux, 2017).

https://doi.org/10.5194/egusphere-2025-4004
Preprint. Discussion started: 29 September 2025

In arid and semi-arid regions, irrigation, precipitation infiltration, and evaporation at the soil-air interface represent the primary forms of soil water transport (Lin et al., 2023). The dynamic water processes, evident through shifts in the isotope signals of soil water, are referred to as the "memory effect" and are crucial for tracking climate and soil hydrology dynamics (Kleine et al., 2020). Changes in stable isotopes in near-surface soil water reflect variations in precipitation, but these changes diminish with depth unless preferential flow exists (Allison and Barnes, 1983). Evaporation mainly occurs at the soil surface (0-10 cm), leading to the enrichment of heavy isotopes (^{2}H and ^{18}O) in the upper soil layer (Liu et al., 2018). To quantify the intensity of evaporative fractionation, researchers have introduced the concepts of deuterium excess (d-excess) and linear excess (lc-excess) (Dansgaard, 1964; Zhu et al., 2022b). Compared to d-excess, lc-excess offers a better explanation of the evaporative fractionation process, primarily because the climatic excesses of precipitation and soil moisture vary smoothly with relatively minor seasonal variations (Landwehr et al., 2014).

Previous studies have primarily focused on the effects of vegetation types on soil moisture storage, transport, and mixing within the same or different climatic zones (Mahindawansha et al., 2019; Turan, 2022). However, relatively few studies have explored the water dynamics in arid irrigated areas, particularly in sprinkler-irrigated rangelands, and their impacts on the regional water cycle. Sprinkler irrigation, as an efficient method of water utilization, plays a crucial role in enhancing regional water resources, promoting vegetation restoration, and supporting the development of

https://doi.org/10.5194/egusphere-2025-4004
Preprint. Discussion started: 29 September 2025

animal husbandry. Therefore, gaining an in-depth understanding of the hydrological processes of vegetation in arid irrigated areas and elucidating the regulatory role of vegetation in the water cycle can aid in better adapting to the impacts of climate change on the hydrological cycle of the source area.

In this study, we focused on sprinkler-irrigated pasture in a typical arid irrigated area sprinkler irrigation significantly alters soil water dynamics, with vertical transport dominating and evaporation being a major loss pathway.and applied stable isotope techniques to investigate its water storage, migration, and mixing processes. The specific objectives were: (1) to understand the dynamics of water storage and isotopic changes in sprinkler-irrigated pastureland across different soil depths; (2) to explore the mechanisms of water migration within the soil profile and identify key influencing factors; and (3) to quantify evaporation losses and assess the efficiency of sprinkler irrigation in arid regions. The results of this study will provide a scientific basis for water resource management and ecosystem protection in arid zones, while also offering new perspectives for studying the regional water cycle in the context of climate change adaptation.

2. Materials and methods

2.1 Study area

The Jingtaichuan Power Lift Irrigation Project in Gansu Province, known as the Jingdian Irrigation Area, is located at the junction of Gansu, Ningxia, and Inner Mongolia provinces (regions) in China (37°26′-38°41′N, 103°33′-104°43′E), covering a total area of 1,496 km². The first phase of the irrigation district was completed in

https://doi.org/10.5194/egusphere-2025-4004
Preprint. Discussion started: 29 September 2025

1971, with the second phase becoming operational in 1987; this study primarily focuses on the area irrigated during the first phase (Fig. 1). The region's climate is classified as temperate continental semi-arid, with an average annual precipitation of 200 mm, most of which falls between May and September, and a multi-year average evapotranspiration of 2,365.9 mm (Wang et al., 2007). The area is characterized by arid conditions and low rainfall, a significant temperature variation between day and night, strong evapotranspiration, long periods of sunshine, windy springs, hot summers, and an extended frost-free period.

The irrigation area extends from east to west, encompassing typical hydrogeological units such as the closed Baidunzi-Manshuitan Basin, the semi-open Zhitan, and the open Haizitan-Yanghuzitan. Within the Jingdian Irrigation District, cultivated land is primarily located in the pre-mountain alluvial floodplain inclined plains, with the overall topography sloping from southwest to northeast. The cultivated soil in this area is predominantly desert gray calcareous, with a texture mainly consisting of sandy loam and light loam. The soil surface has minimal crusting, low organic matter content, and a loose structure. It features numerous capillary pores with good continuity, facilitating the transport of salts and water. The primary crops grown in the irrigation area include wheat, corn, wolfberry, and potato (Li et al., 2020).

https://doi.org/10.5194/egusphere-2025-4004
Preprint. Discussion started: 29 September 2025

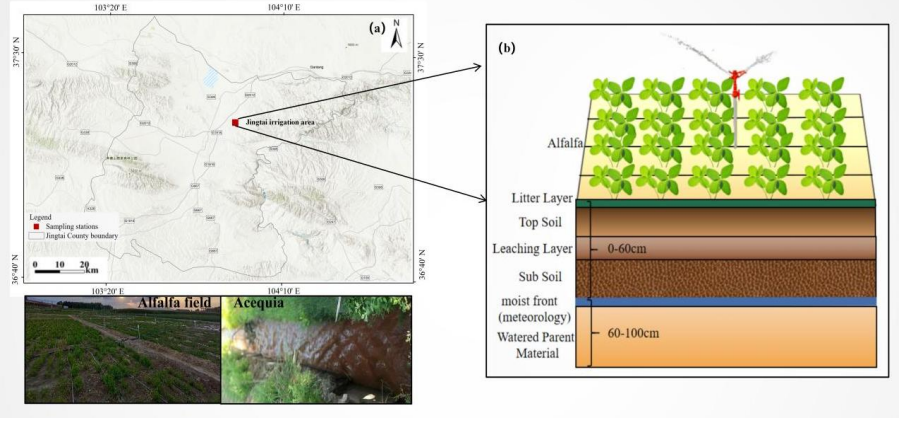

Fig. 1. Study area at the Jingtai Experimental Station in Northwest China. (a) Jingtai experimental field; (b) Representative soil profile.

2.2 Plotting and Sample Collection

In this study, samples of atmospheric precipitation, soil water, groundwater, and sprinkler irrigation water were collected from the experimental field during the alfalfa growth period, spanning from May to September in 2021 and 2023, respectively.

2.2.1 Collection of soil samples

Soil samples were collected from the experimental field at depths of 0-10, 10-20, 20-30, 30-40, 40-50, 50-60, 60-70, 70-80, 80-90, and 90-100 cm. Sampling occurred once before sprinkler irrigation and for five consecutive days afterwards. For each soil layer, four parallel samples were taken. Three samples were placed in 50 ml glass bottles, sealed with laminating film on the caps, labeled with the date and sampling depth, and then frozen for transportation to the Oasis Resource and Sustainability Laboratory at Northwest Normal University for cold storage. The fourth parallel sample was placed in a 100g aluminum box, weighed, recorded, and stored for laboratory analysis of soil moisture content and bulk density.

https://doi.org/10.5194/egusphere-2025-4004
Preprint. Discussion started: 29 September 2025

Table 1. Texture and moisture content of the experimental field soil profile (0-100cm)

Soil depth（cm）	Clay (%)	Silt (%)	Sand (%)	Soil moisture(%)
0-10	9.24	37.26	48.32	90.42
10-20	10.65	36.49	47.01	90.91
20-30	9.37	43.21	43.28	91.32
30-40	11.25	37.19	45.72	86.79
40-50	10.72	34.27	50.31	85.42
50-60	10.67	41.09	43.08	84.61
60-70	9.43	41.31	44.19	91.39
70-80	10.08	37.29	46.92	91.46
80-90	10.64	36.30	49.01	90.69
90-100	6.31	34.29	54.25	91.57

2.2.2 Sampling collection of irrigation water

Sprinkler water was collected during each irrigation event using 80 ml high-density polyethylene sample bottles. After collection, the bottles were sealed with laminating film and kept frozen until they were needed for analysis.

2.2.3 Precipitation sample collection

In the designated collection area, a Chinese Standard Precipitation Gauge (CSPG) was installed, measuring 70 cm in height and 20 cm in width, with an accuracy of 0.1 mm. A 20 cm diameter funnel was mounted on top for rainwater collection. To prevent isotope fractionation, a polyethylene anti-evaporation device was placed at the funnel's outlet. Professionally trained local farmers were responsible for collecting precipitation samples. To minimize analytical errors from sample evaporation, samples were collected immediately after precipitation events and transferred to 100 ml high-density polyethylene (HDPE) bottles (Zhu et al., 2022a). Each collection included three parallel samples, which were sealed with a fiber membrane and refrigerated at 4°C for subsequent analysis. A total of 110 precipitation samples were

https://doi.org/10.5194/egusphere-2025-4004
Preprint. Discussion started: 29 September 2025

collected in 2021 and 2023 during the May to September observation periods.

2.2.4 Groundwater sample collection

Groundwater samples were collected from farmers' wells near the experimental field using 100 ml high-density polyethylene sample bottles. The bottles were sealed with a sealing film and immediately capped to prevent evaporation. The samples were then placed in a portable ice box maintained at 4°C and transported back to the laboratory, where they were kept refrigerated until needed for experimental measurements.

2.2.5 Meteorological data

During the sampling period, local meteorological data, including temperature and relative humidity, were obtained and recorded using an automatic weather station (WatchDog 2000 series) installed near the sampling site.

2.3 Sample analysis

Sample analysis and determination were conducted at the Isotope Laboratory, School of Geography and Environmental Science, Northwest Normal University. Soil water was extracted using a fully automated low-temperature vacuum condensation extraction system (LI-2100, LICA United Technology Limited, China). During extraction, the temperature was set at 180°C, the vacuum at 1200 Pa, and the duration was 150 minutes. All water samples were analyzed using a liquid water isotope analyzer (DLT-100, Los Gatos Research, USA). Each sample and isotope standard was injected sequentially six times using a microliter syringe. To minimize experimental errors, the first two injection values were discarded, and the average of

https://doi.org/10.5194/egusphere-2025-4004
Preprint. Discussion started: 29 September 2025

the last four injections was taken as the final value. Three parallel soil water samples were also measured and averaged separately. The derived $\delta^{2}H$ and $\delta^{18}O$ values were expressed as parts per thousand (‰) differences from the mean value, conforming to the Vienna Standard Mean Ocean Water (VSMOW) standard.

$$\delta = \left(\frac{R_{sample}}{R_{\text{standard}}} - 1 \right) \times 1000‰ \quad (1)$$

where R_{sample} is the ratio of $^{18}O/^{16}O$ or $^{2}H/^{1}H$ in the samples and $R_{standard}$ is the ratio of $^{18}O/^{16}O$ or $^{2}H/^{1}H$ in V-SMOW. The precision was ± 0.6‰ for $\delta^{2}H$ and ± 0.2‰ for $\delta^{18}O$.

2.4 Analytical methods

2.4.1 potential vaporization

Potential evapotranspiration (PET) was calculated according to the Penman-Monteith equation (Allen, 1998):

$$PET = \frac{0.408\Delta(R_n - G) + \gamma \frac{900}{T + 273} u^2 (e_s - e_a)}{\Delta + \gamma(1 + 0.34u^2)} \quad (2)$$

where PET is the potential daily evapotranspiration (mmd^{-1}), R_n is the net radiation (MJ m^2 d^{-1}), G is the soil heat flux density (MJ m^2 d^{-1}), γ is the humidity constant ($kPa^{\circ -1}$), u_2 is the wind speed at a height of 2 m (ms^{-1}), T is the average daily air temperature at 2 m height (◦), l is the slope of the vapor pressure curve ($kPa^{\circ -1}$), e_a is the actual vapor pressure (kPa), and e_s is the saturated vapor pressure (kPa). These data were obtained from nearby weather stations.

2.4.2 Lc-excess

Defining the linear relationship between $\delta^{2}H$ and $\delta^{18}O$ in precipitation and soil

https://doi.org/10.5194/egusphere-2025-4004
Preprint. Discussion started: 29 September 2025

water as the local meteorological water line (LMWL) and soil water line (SWL), respectively, is important for studying the evaporative fractionation of stable isotopes in the water cycle. We further calculated the excess for each soil water and precipitation sample. The LMWL excesses for different water bodies can characterize the evapotranspiration index of different water bodies relative to local precipitation (Landwehr and Coplen, 2004):

$$lc-excess = \delta^2 H - a \times \delta^{18} O - \mathrm{b} \quad (3)$$

a and b are the slope and intercept of the meteorological water line (LMWL), respectively, and δ^2H and δ^{18}O are the isotope values of hydrogen and oxygen in the collected soil samples. The physical significance of the excess surplus is expressed as the degree of deviation of the isotope values in the samples from the LMWL, indicating a non-equilibrium dynamic fractionation process caused by evaporation. In general, the variation of local precipitation excess is mainly influenced by different water vapor sources, with an annual mean value of 0. Since stable isotopes in soil water are enriched by evaporation, the mean LMWL excess is usually negative. (Landwehr et al., 2014; Sprenger et al., 2016)

2.4.3 Soil water storage

Soil water storage is the thickness of the water layer formed by all the water in a given soil layer (Milly, 1994) and is expressed by the following equation:

$$S = R \times W \times H \times 10 \quad (4)$$

Where S is the amount of soil water in a thickness layer (mm), R is the soil bulk density (g cm^{-3}) and H is the soil thickness (cm). The weight water content W is

https://doi.org/10.5194/egusphere-2025-4004
Preprint. Discussion started: 29 September 2025

expressed by the following equation:

$$W = \frac{M_1 - M_2}{M_2} \times 100\% \quad (5)$$

Where M_1 is the weight value of wet soil (g) and M_2 is the weight value of dry soil (g).

2.4.5 Infiltration of irrigation water

Infiltration of soil water can be estimated based on the soil water balance combined with the conservation of isotopic mass (Yang et al., 2015). If it is assumed that the water storage capacity (W_a) of the soil layer after sprinkler irrigation consists of the water demand (W_b) and infiltration water (W_i) of the same layer before sprinkler irrigation, the equation is as follows:

$$W_a = W_b + W_i \quad (6)$$

Based on the isotopic mass balance, we obtain the following:

$$\delta_a W_a = \delta_b W_b + \delta_i W_i \quad (7)$$

where δ_a, δ_b, and δ_i denote $\delta^{18}O$ as described above. rearranging the above equations:

$$\frac{W_i}{W_a} = \left(\frac{\delta_a - \delta_b}{\delta_i - \delta_b} \right) \times 100\% \quad (8)$$

Therefore, the amount of water infiltrated by sprinkler irrigation water into each soil layer can be quantified by $\delta^{18}O$ of different compositions and W_a.

3. Results

3.1 Isotopic characterization of soil moisture

The values of δ^2H and $\delta^{18}O$ of soil water varied considerably during the

https://doi.org/10.5194/egusphere-2025-4004
Preprint. Discussion started: 29 September 2025

observation period and their mean values were -71.93±6.61‰ and -9.50±1.18‰, respectively. The mean values of δ^2H and $\delta^{18}O$ of atmospheric precipitation were -54.30±9.61‰; -10.90±1.18‰ (Table 2), respectively (Fig. 2). The slope of the irrigation water line (IML) may be higher than the global meteorological line (GMWL) due to high temperatures during the growing season, indicating the effectiveness of anthropogenic interventions in water supply to the farmland.The slope and intercept of the SWL are smaller than those of the LMWL, suggesting that soil moisture is affected by evaporation, which enriches soil water isotopes, but some of the isotope values exceeded those of the LMWL, further suggesting that rain water is not the only addition to the soil water source (Fig. 3).

https://doi.org/10.5194/egusphere-2025-4004
Preprint. Discussion started: 29 September 2025

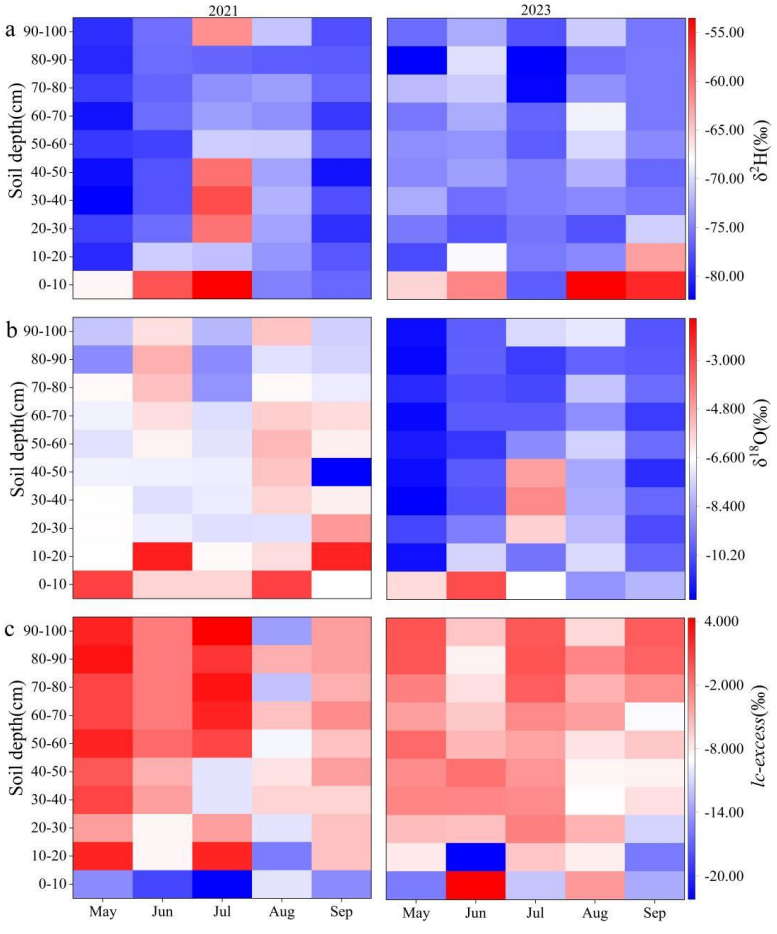

Fig. 2. Vertical distribution heat map of soil water δ2 H (a), δ18O (b), lc-excess (c) at a depth of 0–100 cm during the growth period of plantation.

We did not observe significant precipitation input signals in the soil water isotopes. This can be attributed to a couple of reasons. Firstly, the Jingtai irrigation area is an arid region with low precipitation and strong surface evaporation. Consequently, most rainwater falls on the surface of the mulch and evaporates rapidly, with only a small amount infiltrating the soil and mixing with the existing pore water. Secondly, during sprinkler irrigation, a substantial amount of water infiltrates the soil

https://doi.org/10.5194/egusphere-2025-4004
Preprint. Discussion started: 29 September 2025

through pore spaces, and its impact on soil water isotopes masks the precipitation input.The temporal dynamics of the sprinkler irrigation water input signal are generally reflected in the soil water isotope data. Before sprinkler irrigation, the dry conditions led to the enrichment of soil moisture $\delta^{2}H$ and $\delta^{18}O$ through fractionation. Since the sprinkler irrigation water originates from the Yellow Diversion Irrigation Canal, its stable hydrogen and oxygen isotopic compositions are significantly lower relative to the shallow soil water. During irrigation, the infiltrated water mixed with the existing soil pore water, imparting its isotopic signature to the soil and gradually reducing it. This effect was particularly evident in the topsoil. About a week after sprinkler irrigation, evaporation caused dynamic fractionation of isotopes in the soil, and the isotopic composition of the soil water gradually returned to its pre-sprinkler state after some time.

Enrichment of soil moisture isotopes during alfalfa's growth period was accompanied by a decrease in SW (soil moisture) lc-excess ($r = -0.55$, $p < 0.01$, δ2H; $r = -0.83$, $p < 0.01$, δ18O). low values of SWlc-excess corresponded to isotope enrichment. Sprinkler irrigation depleted the isotopes initially enriched in the surface soil and lost the fractionation signal. The range of SWlc-excess controlled by evaporation was relatively large (-19.2‰ to 5.12‰) before sprinkler irrigation, and the range of SWlc-excess during sprinkler irrigation decreased significantly (-6.7‰ to 7.0‰). With the continued effect of fractionation after the completion of sprinkler irrigation the range of SWlc-excess gradually returned to the pre-sprinkler irrigation level. The soil moisture isotope evaporation signal was not attenuated during

https://doi.org/10.5194/egusphere-2025-4004
Preprint. Discussion started: 29 September 2025

precipitation because the rainwater infiltration was small or the new water was not mixed with the existing soil water. (Fig.2.)

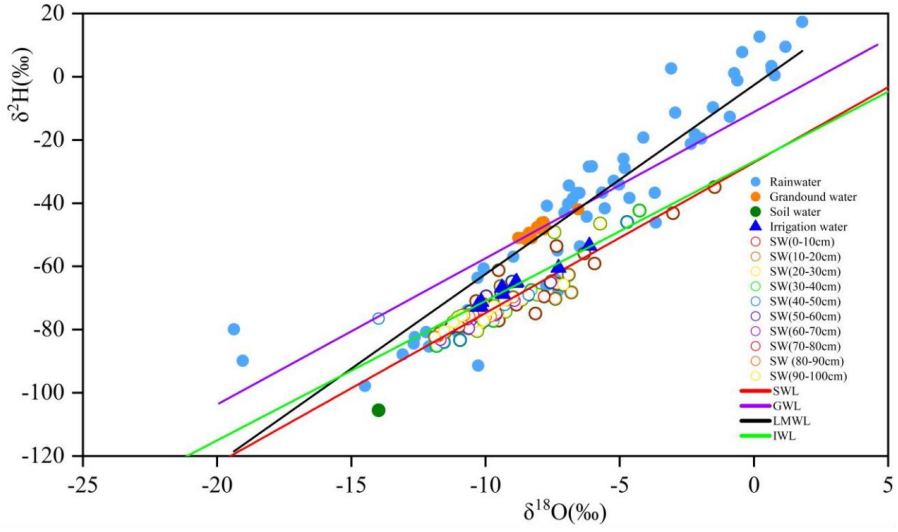

Fig. 3.The depth of the soil samples is shown by different colors in the isotope plot.Relationship between δ2H and δ18O of soil water during alfalfa growing season.

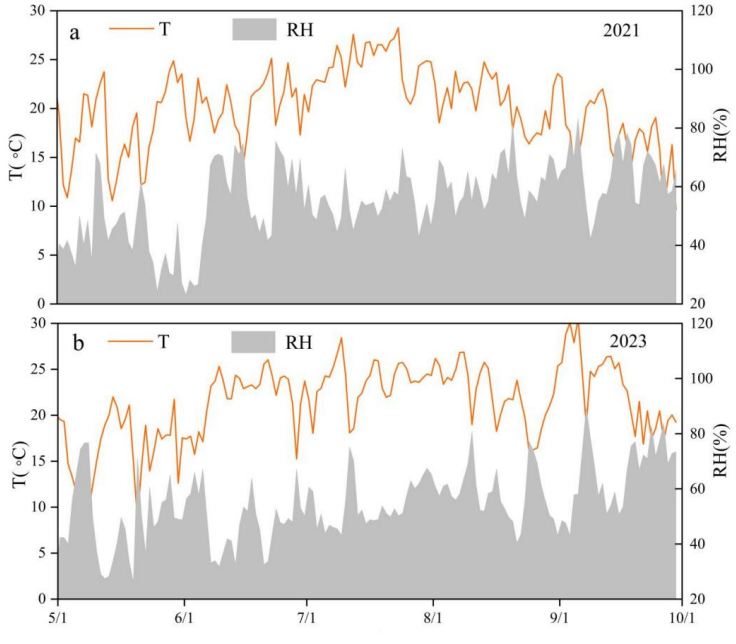

https://doi.org/10.5194/egusphere-2025-4004
Preprint. Discussion started: 29 September 2025

Fig. 4. Study the meteorological and hydrological conditions (a, b. Temperature and relative humidity data for the years 2021 and 2023)

3.2 Soil moisture storage dynamics

In this study, water storage in the 0-40 cm soil layer of the study area was calculated throughout the observation period using soil water measurements. It was found that water storage in the alfalfa soil gradually decreased from May to July, ranging from 133.4 mm to 112.1 mm, and then increased from July onwards, reaching 142.8 mm. The average monthly water storage was lowest in the 0-10 cm layer (24.6 mm) and highest in the 30-40 cm layer (37.4 mm). The surface soil, being directly affected by evapotranspiration, loses water more quickly and has a looser structure, leading to a weaker water storage capacity. In general, the water storage capacity of the 0-10 cm soil layer is smaller than that of the deeper layers. (Fig. 5)

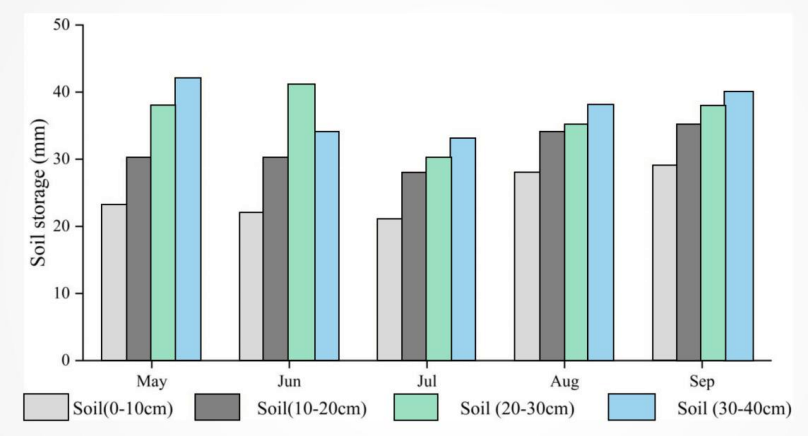

Fig. 5 Monthly variation of soil water storage in 0-40cm soil layer.

3.3 Vertical and horizontal water transport patterns

When sprinkler irrigation begins, water droplets fall on the soil surface, filling micropores and cracks. At this point, water movement is primarily driven by gravity

https://doi.org/10.5194/egusphere-2025-4004
Preprint. Discussion started: 29 September 2025

and capillary forces, causing it to move downward. The water content in the 0-10 cm soil layer increases significantly compared to pre-irrigation levels. As sprinkler irrigation continues, water gradually infiltrates deeper, forming a wetting front, with dry soil below and wet soil above. During this stage, the infiltration rate is typically high due to the soil's strong water absorption capacity.

Over time, the wetting front reaches a depth of 50-60 cm, and the infiltration rate begins to stabilize. At this stage, the infiltration rate is influenced by factors such as soil type, structure, porosity, and the rate of sprinkler irrigation. If the sprinkler irrigation continues for too long, causing soil pores to become completely saturated, the infiltration rate will decrease, potentially leading to surface runoff. Excess water that cannot infiltrate promptly may form puddles on the soil surface. (Fig. 6)

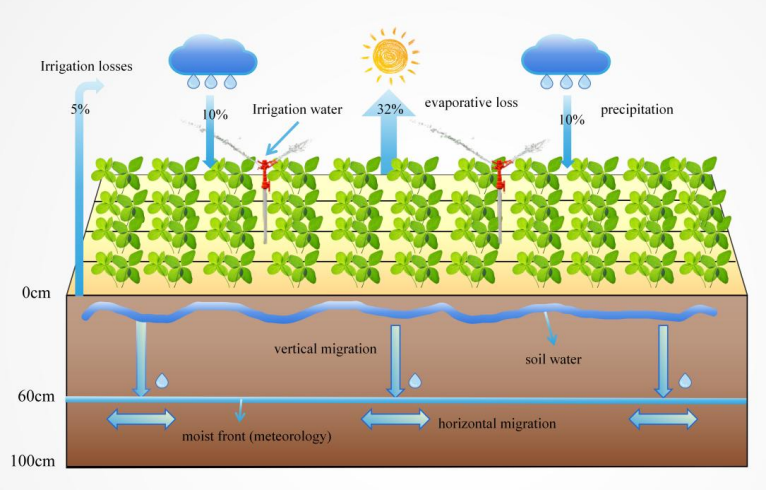

Fig. 6 Conceptual map of water transport in irrigation pastures

As moisture infiltrates vertically, it also moves horizontally along the soil profile. This horizontal migration is driven by spatial variability in soil porosity and permeability. During sprinkler irrigation, moisture forms a wetting front at the soil

https://doi.org/10.5194/egusphere-2025-4004
Preprint. Discussion started: 29 September 2025

surface, and within this front, moisture infiltrates laterally into drier soil areas on either side. Below the wetting front, the lateral movement of moisture is slower, resulting in a wider zone of wetness. This lateral expansion enhances the uniformity of moisture distribution within the soil.

Table 2. General characteristics of precipitation δ2H and δ18O in different areas from May to Septmber 2021 and 2023.

Different waters	Soil depth(cm)	δ^2H/‰				$\delta^{18}O$/‰			
		Max	Min	Mean	SD	Max	Min	Mean	SD
Rain water		-12.61	-79.58	-54.30	27.20	-1.70	-19.30	-10.90	2.80
Irrigation water		-53.47	-72.80	-66.87	16.80	-6.10	-10.20	-9.08	2.40
Soil water	0-10	-34.91	-77.15	-59.75	9.75	-1.46	-9.51	-6.74	1.27
	10-20	-62.69	-80.84	-71.74	8.25	-6.80	-11.50	-8.92	1.38
	20-30	-46.45	-80.45	-72.59	6.35	-5.73	-10.58	-9.42	1.02
	30-40	-42.30	-85.17	-72.34	4.69	-4.26	-11.82	-9.49	0.98
	40-50	-45.91	-83.94	-73.08	3.54	-4.72	-13.98	-10.00	0.86
	50-60	-64.80	-79.44	-73.31	7.32	-7.57	-11.29	-9.84	0.02
	60-70	-68.67	-83.24	-74.66	5.62	-8.92	-11.68	-10.09	1.04
	70-80	-69.52	-81.99	-74.34	5.49	-7.81	-11.76	-10.04	1.24
	80-90	-69.72	-82.39	-75.54	5.27	-0.28	-11.88	-10.61	1.07
	90-100	-49.16	-80.59	-71.93	6.38	-7.43	-11.53	-9.81	1.15
	0-100(cm)	-34.91	-85.17	-71.93	6.59	-0.28	-13.98	-9.50	1.09

3.4 Mixing process of moisture from different sources

Changes in soil water isotopes and soil moisture can be used to trace the input and mixing processes of water from various sources in vegetation. In the study area, precipitation is low, and irrigation mainly relies on water from the Yellow Irrigation Canal for sprinkler irrigation of pastureland. Following irrigation to enhance water availability, the soil becomes moist, allowing water to move rapidly from exposed soil fissures and root systems through the soil matrix into deeper layers. This rapid movement results in a sudden depletion of soil isotopes at depths of 60-100 cm due to

https://doi.org/10.5194/egusphere-2025-4004
Preprint. Discussion started: 29 September 2025

the preferential infiltration of recently depleted irrigation water reaching these depths quickly.After a brief period of reduced evaporation, the soil rewets due to sprinkler irrigation infiltration. Soil moisture content in the 0-100 cm soil layer remains above 10 mm per month (Fig.3). From mid-May to late August, precipitation in the study area increases compared to earlier in the year (Fig.4)

Soil moisture evaporated rapidly with rising temperatures. Following sprinkler irrigation, the soil was re-wetted, and soil water isotopes were replaced and mixed with irrigation water and groundwater. The isotope values of soil water were consistently located in the lower right of the Irrigation Water Line (IWL), indicating that soil water was primarily recharged by irrigation water. The results demonstrated that water in the 0-60 cm soil layer of the pasture was mainly derived from irrigation, while in the 60-100 cm soil layer, irrigation water mixed with groundwater. (Fig.5)

https://doi.org/10.5194/egusphere-2025-4004
Preprint. Discussion started: 29 September 2025

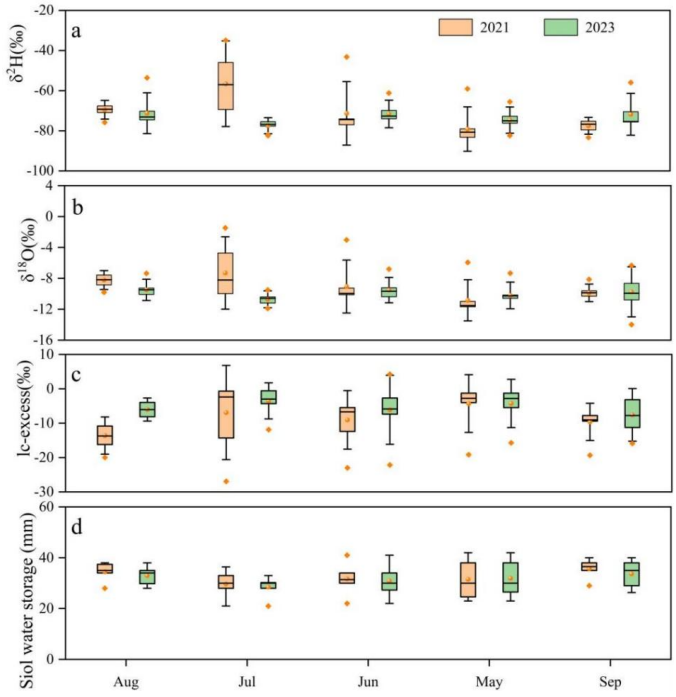

Fig. 7.Variation of soil water δ^2H (a), $\delta^{18}O$ (b), lc-excess (c) and soil water storage (d) during the plantation growth period (The horizontal line in the box diagram represents the median, and the square box represents the average).

4. Discussions

4.1 Factors affecting water storage, migration and mixing processes

Soil water storage is a crucial indicator for assessing the capacity of ecosystems for water resource conservation and soil conservation. It reflects the potential of soils to regulate and buffer water (Milly et al., 1993). Greater water storage indicates a higher potential of the soil to regulate rainfall redistribution (Xia et al., 2017). Grazing pastures exhibit the highest water storage capacity in the topsoil, primarily due to the dense root network formed by high-density grass vegetation, shallow root distribution, and root development within the topsoil (Ferrante et al., 2014).

https://doi.org/10.5194/egusphere-2025-4004
Preprint. Discussion started: 29 September 2025

Climatic conditions, such as temperature, precipitation, and wind speed, directly influence soil moisture evaporation and plant transpiration. Soil properties, including texture, structure, and porosity, play a decisive role in water infiltration, storage, and movement.Vegetation type and root distribution significantly impact water uptake and utilization. Irrigation practices directly affect the distribution and transport of soil moisture. Additionally, groundwater dynamics, including the water table and flow, are key factors in the water cycling process.The interaction of these factors reveals the complexity of the water cycle and provides a theoretical foundation for developing scientific water resource management and ecological protection strategies.

4.2 Influence of water mixing process on water utilization of pasture grasses

The mixing process plays a crucial role in pasture water utilization, influencing both the efficiency of water acquisition by plants and the overall water balance of the ecosystem. This study found that the integration of different water sources—sprinkler water, groundwater, and soil water—significantly affects the water utilization of forage. By effectively mixing these sources, the pasture can optimize water availability for plant growth and maintain a balanced ecosystem.

The isotopic compositions of different water sources change during the mixing process, potentially influencing the uptake preference of water by plant roots and subsequently affecting the plant's water utilization strategy (Jiao et al., 2023). Additionally, the mixing process enhances water availability within the soil profile, helping to alleviate drought stress and improve the drought tolerance of forages. However, inappropriate mixing can lead to deep water leakage or evaporative loss,

https://doi.org/10.5194/egusphere-2025-4004
Preprint. Discussion started: 29 September 2025

thereby reducing water utilization efficiency. Consequently, understanding the effects of mixing processes on pasture water use is vital for developing effective irrigation strategies, optimizing vegetation layout, and enhancing water management efficiency.

4.3 Implications of stable isotope-based understanding for water management in sprinkler-irrigated pastures

Under sprinkler irrigation, we observed that the uniformity of soil water content was significantly better compared to surface irrigation. As the uniformity of sprinkler irrigation improved, so did the uniformity of soil water content. However, different irrigation patterns did not significantly affect soil water content. In terms of soil water distribution, the most significant increase in water content occurred in the 0-10 cm soil layer during sprinkler irrigation. Within 24 hours following the cessation of sprinkler irrigation, water movement in the 0-30 cm soil layer was more active, with an increase in water content that then stabilized.

By 72 hours post-irrigation, the size of the wetted soil area and the water movement process had largely stabilized. Nine days after the conclusion of sprinkler irrigation, both soil moisture and isotopic characteristics returned to their pre-irrigation states. At high sprinkler intensities, using intermittent sprinkler irrigation and increasing the number and duration of intervals can help reduce the risk of surface runoff and deep seepage to some extent (Fig. 7).

This study reveals the complexity of water storage, migration and mixing processes in sprinkler-irrigated pastures and proposes a series of management strategies based on this understanding. In order to improve water use efficiency and

https://doi.org/10.5194/egusphere-2025-4004
Preprint. Discussion started: 29 September 2025

safeguard the sustainability of the ecosystem, the following measures are recommended: implementing precision sprinkler irrigation and adjusting the sprinkler program according to soil moisture monitoring data and plant water demand patterns; improving soil properties to enhance its water retention capacity; rationally selecting vegetation to improve water use efficiency; utilizing topographic features to reduce soil erosion; and establishing and maintaining a comprehensive moisture monitoring system to provide management decisions with provide real-time data support. These comprehensive measures will help to ensure that the water management of pastureland is scientific and rational, while maintaining the stability of ecohydrological processes.

5. Conclusions

In this study, we used the stable isotope technique to investigate in depth the water storage, transport and mixing processes in sprinkler-irrigated pastureland. The results showed that the isotopic characteristics of soil moisture changed significantly after irrigation, and both soil moisture and isotopic characteristics returned to the pre-irrigation state after an average of 9 days. Moisture was mainly transported vertically in the soil, with a low percentage of horizontal transport. Evapotranspiration losses due to sprinkler irrigation accounted for 32%, while losses due to over-irrigation (infiltration into the soil layer below 60 cm) accounted for 5%.

Our study reveals the complexity of water dynamics in sprinkler-irrigated pastures in the arid zone, emphasizing the effectiveness of sprinkler irrigation in controlling infiltration losses, but also pointing out the significance of evaporation

https://doi.org/10.5194/egusphere-2025-4004
Preprint. Discussion started: 29 September 2025

losses. We recommend the promotion of low-level multipoint sprinkler irrigation and nighttime sprinkler irrigation patterns to improve water use efficiency and ensure agricultural sustainability. This study provides a comprehensive understanding of water dynamics in sprinkler-irrigated pastureland, emphasizing the role of evaporation and vertical water transport. The findings support the adoption of low-level multipoint sprinkler irrigation and nighttime irrigation to enhance water use efficiency in arid regions. This research contributes to the broader understanding of eco-hydrological processes and offers practical insights for sustainable water management in the context of climate change.

Acknowledgments

This research was financially supported by the National Natural Science Foundation of China(42371040, 41971036), the Key Natural Science Foundation of Gansu Province(23JRRA698), the Key Research and Development Program of Gansu Province(22YF7NA122), the Cultivation Program of Major key projects of Northwest Normal University(NWNU-LKZD-202302), the Oasis Scientific Research achievements Breakthrough Action Plan Project of Northwest Normal University(NWNU-LZKX-202303).

Data Availability Statement

Data will be made available on request.

Author contributions statement

JY: Writing-Original draft preparation; XQ,ZZ and YJ: Visualization; WL and RL: Investigation; GZ: Supervision; YG: Software.

https://doi.org/10.5194/egusphere-2025-4004
Preprint. Discussion started: 29 September 2025

Declaration of Interest Statement

We undersigned declare that this manuscript entitled "Moisture storage, transport and mixing processes after sprinkler irrigation of pastureland: a stable isotope-based isotope understanding" is original, and has not been published before and is not currently being considered for publication elsewhere.

The authors declare that they have no known competing financial interests or personal relationships that could have appeared to influence the work reported in this paper.

References

Allen, R. G., Pereira, L. S., Raes, D., & Smith, M. (1998). Crop evapotranspiration-Guidelines for computing crop water requirements-FAO Irrigation and drainage paper 56. Fao, Rome, 300(9), D05109.

Allison, G.B., Barnes, C.J., 1983. Estimation of evaporation from non-vegetated surfaces using natural deuterium. Nature 5896 (301), 143–145.

Chen X, Deng W, Xiao H, et al.,2024 A Perspective on Probing Coral Resilience to Climate and Environmental Changes Using Stable Isotopes of Bio-Utilized Metal Elements[J]. Journal of Geophysical Research: Biogeosciences, 129(1):

Dansgaard, W. (1964). Stable isotopes in precipitation. tellus,16(4), 436-468.

Duvert, C., Stewart, M. K., Cendón, D. I., and Raiber, M.,2016 Time series of tritium, stable isotopes and chloride reveal short-term variations in groundwater contribution to a stream, Hydrol. Earth Syst. Sci., 20, 257–277.

Ferrante, D., Oliva, G.E., Fern´andez, R.J., 2014. Soil water dynamics, root systems, and plant responses in a semiarid grassland of Southern Patagonia. J. Arid Environ. 104, 52–58.

https://doi.org/10.5194/egusphere-2025-4004
Preprint. Discussion started: 29 September 2025

458 Gibson, J. J., Holmes, T., Stadnyk, T. A., Birks, S. J., Eby, P., & Pietroniro, A.
459 (2021). Isotopic constraints on water balance and evapotranspiration partitioning in
460 gauged watersheds across Canada. Journal of Hydrology: Regional Studies, 37,
461 100878.

462 Jiao, Y., Zhu, G., Meng, G., Lu, S., Qiu, D., Lin, X., ... & Sun, N.,2023
463 Estimating non-productive water loss in irrigated farmland in arid oasis regions:
464 Based on stable isotope data. Agricultural Water Management, 289, 108515.

465 Kleine, L., Tetzlaff, D., Smith, A., Wang, H., and Soulsby, C.,2018 Using water
466 stable isotopes to understand evaporation, moisture stress, and re-wetting in
467 catchment forest and grassland soils of the summer drought of, Hydrol. Earth Syst.
468 Sci., 24, 3737–3752,

469 Koeniger, P., Gaj, M., Beyer, M., and Himmelsbach, T.,2016 Review on soil
470 water isotope-based groundwater recharge estimations, Hydrol. Process., 30, 2817–
471 2834.

472 Landwehr, J. M., Coplen T. B., 2004. Line-conditioned excess: a new method for
473 characterizing stable hydrogen and oxygen isotope ratios in hydrologic systems.

474 Landwehr, J. M., Coplen, T. B.,2014 and Stewart, D. W. Spatial, seasonal, and
475 source variability in the stable oxygen and hydrogen isotopic composition of tap
476 waters throughout the USA, Hydrol. Process, 28, 5382–5422,

477 Li J, Fei L, Li S, et al.,2020 Development of “water-suitable” agriculture based
478 on a statistical analysis of factors affecting irrigation water demand[J]. Science of The
479 Total Environment, 744: 140986.

https://doi.org/10.5194/egusphere-2025-4004
Preprint. Discussion started: 29 September 2025

Lin X, Zhu G, Qiu D, et al.,2023. Stable precipitation isotope records of cold wave events in Eurasia[J].Atmospheric Research,:107070.

Liu, Y., Miao, H., Huang, Z., et al., 2018. Soil water depletion patterns of artificial forest species and ages on the Loess Plateau (China). For. Ecol. Manage. 417, 137–143.

Mahindawansha, A., Külls, C., Kraft, P., et al., 2019. Estimating water flux and evaporation losses using stable isotopes of soil water from irrigated agricultural crops in tropical humid regions. Hydrol. Earth Syst. Sci. Discuss. (June) 1–28.

Milly, P.C.D., 1993. An analytic solution of the stochastic storage problem applicable to soil water. Water Resour. Res. 29 (11), 3755–3758.

Milly, P.C.D., 1994. Climate, soil water storage, and the average annual water balance. Water Resour. Res. 30 (7), 2143–2156.

Rothfuss, Y. and Javaux, M.,2017. Reviews and syntheses: Isotopic approaches to quantify root water uptake: a review and comparison of methods, Biogeosciences, 14, 2199–2224.

Sprenger, M., Leistert, H., Gimbel, K.,et al.,2016. Illuminating hydrological processes at the soil-vegetation-atmosphere interface with water stable isotopes. Rev. Geophys. 3 (54), 674–704.

Turan, V., 2022. Calcite in combination with olive pulp biochar reduces Ni mobility in soil and its distribution in chili plant. Int. J. Phytoremediat. 24 (2), 166–176.

Wang, Z., Chen, R., Li, W., Zhang, J., Zhang, J., Song, L., ... & Guo, L. (2024).

https://doi.org/10.5194/egusphere-2025-4004
Preprint. Discussion started: 29 September 2025

502 Mulched drip irrigation: a promising practice for sustainable agriculture in China's
503 arid region. npj Sustainable Agriculture, 2(1), 17.

504 Wang, Y., Xue, C.D., Fan, J.L., 2007. Discussion on water saving measures and
505 ways of water lifting irrigation from the current situation and soil resources in
506 Jingdian Irrigation District. J. Irrig. Drain. 26 (4B), 198–199.

507 Xia, J., Zhao, Z., Fang, Y., 2017. Soil hydro-physical characteristics and water
508 retention function of typical shrubbery stands in the Yellow River delta of China.
509 Catena 156, 315–324.

510 Xiao, W., Wei, Z., and Wen, X., 2018. Evapotranspiration partitioning at the
511 ecosystem scale using the stable isotope method – A review, Agr. Forest Meteorol.,
512 263,346–361.

513 Xu, Z., Chen, X., Liu, J., Zhang, Y., Chau, S., Bhattarai, N., & Li, Y. (2020).
514 Impacts of irrigated agriculture on food – energy – water – CO2 nexus across
515 metacoupled systems. Nature communications, 11(1), 5837.

516 Yang, B., Wen, X., Sun, X., 2015. Irrigation depth far exceeds water uptake
517 depth in an oasis cropland in themiddle reaches of Heihe River Basin. Sci. Rep. 5,
518 15206.

519 Zaitchik, B. F., Rodell, M., Biasutti, M., & Seneviratne, S. I. (2023). Wetting and
520 drying trends under climate change. Nature Water, 1(6), 502–513.

521 Zhu, G., Yong, L., Zhang, Z., et al., 2021. Effects of plastic mulch on soil water
522 migration in arid oasis farmland: evidence of stable isotopes. Catena 207.

523 Zhu G, Yong L, Zhao X, et al., 2022a Evaporation, infiltration and storage of soil

https://doi.org/10.5194/egusphere-2025-4004
Preprint. Discussion started: 29 September 2025

water in different vegetation zones in the Qilian Mountains: a stable isotope perspective[J]. Hydrology and Earth System Sciences, 26(14)26-3771.

Zhu, G., Liu, Y., Shi, P., et al., 2022b. Stable water isotope monitoring network of different water bodies in Shiyang River basin, a typical arid river in China. Earth Syst. Sci. Data 14 (8), 3773–3789.